On Eddy-Mixed Longshore Currents: Video Observation and 3D Modeling off Grand Popo Beach, Benin

Authors: Marchesiello, Patrick, Almar, Rafael, Benshila, Rachid, Larnier, Stanislas, Castelle, Bruno, et al.

Source: Journal of Coastal Research, 75(sp1) : 408-412

Published By: Coastal Education and Research Foundation

URL: https://doi.org/10.2112/SI75-082.1

Journal of Coastal Research	SI	75	408-412	Coconut Creek, Florida	2016

On Eddy-Mixed Longshore Currents: Video Observation and 3D Modeling off Grand Popo Beach, Benin

Patrick Marchesiello[†], Rafael Almar[†], Rachid Benshila[‡], Stanislas Larnier[††], Bruno Castelle[§] and James C. McWilliams[§§]

[†]IRD-LEGOS
Université Paul Sabatier/CNRS/CNES/IRD
Toulouse, France

[‡]CNRS-LEGOS
Université Paul Sabatier/CNRS/CNES/IRD
Toulouse, France

[††]CNRS-LAAS
Université Paul Sabatier/CNRS/CNES/IRD
Toulouse, France

[§]CNRS-EPOC
Université de Bordeaux/CNRS
Bordeaux, France

[§§]Department of Atmospheric and Oceanic Sciences
University of Califoria at Los Angeles
Los Angeles, CA, USA

www.cerf-jcr.org

www.JCRonline.org

ABSTRACT

Marchesiello, P.; Almar; R.; Benshila; R.; Larnier, S.; Castelle, B., and McWilliams, J.C., 2016. Morphological Change near Artificial Reefs as a Beach Erosion Countermeasure. In: Vila-Concejo, A.; Bruce, E.; Kennedy, D.M., and McCarroll, R.J. (eds.), Proceedings of the 14th International Coastal Symposium (Sydney, Australia). J. Coast. Res., Special Issue, No. 75, pp. 408-412. Coconut Creek (Florida), ISSN 0749-0208.

The link between intrinsic shear-flow instability of longshore currents and their mean cross-shore profiles has long been suggested. Yet, recent investigations give increasing credit to extrinsic wave forcing mechanisms, downplaying the role of shear waves on the observed variability. Our results for Grand Popo beach, Benin, provide an original attempt to map mean longshore currents forced by an oblique swell. A 3D model investigation shows that their broad mean flow and the frequency band of eddy variability are consistent with shear instability, conversion of mean to eddy kinetic energy and eddy mixing of momentum. Their turbulent dynamics do not clearly fit in any classical 2D or 3D paradigms but show large transfer of energy across the wavenumber spectrum, to both larger and smaller scales.

ADDITIONAL INDEX WORDS: *Nearshore processes, video monitoring, 3D modeling.*

INTRODUCTION

In West Africa, the majority of the population and economic activity is concentrated in the coastal zones. These are open sandy coasts facing narrow continental shelves. The local wave climate dominated by high-energy swell traveling from the South Atlantic forces one of the largest littoral drift in the world (Laibi *et al.*, 2014). As a result and because of half a century of destabilizing development, the entire coast experiences rapid erosion with rates reaching 10 m/yr at Cotonou, Benin (Kaki *et al.*, 2011). Therefore, an assessment of anthropogenic and natural factors controlling erosion is needed based on a better understanding and monitoring of longshore currents. To that end, field studies were conducted in 2013 and 2014 at Grand Popo beach, Benin (Figure 1; Almar *et al.*, 2014). The beach presents a longshore-uniform low tide terrace where persistent oblique swells generate strong and narrow longshore currents.

Dominant energy sources in the nearshore are considered to be gravity waves and mean currents. The frequency band between infragravity (~2-10 Hz) and mean flow, called Very Low Frequency (VLF), have been associated with either wave-grouping, surfzone eddies due to vorticity generation by short-crested wave breaking (Clark *et al.*, 2012; Peregrine, 1998), or shear waves and eddies resulting from shear instability of longshore currents (Bowen and Holman, 1989). In many occasions where longshore flow is generated by an oblique swell, VLF motions are seen to be energetic, coherent in the longshore direction and linked to the strength of the mean circulation (Dodd *et al.*, 1992; Noyes *et al.*, 2004; Oltman-Shay *et al.*, 1989).

Linear stability analysis and numerical shallow-water models (*e.g.*, Allen *et al.*, 1996; Bowen and Holman, 1989; Slinn *et al.*, 1998) show that longshore currents are strongly unstable systems (fast growth rate of the most unstable modes). Usual conditions for shear wave resonance is that current profiles have inflection points (change of sign of vorticity gradients) and that frictional spindown $t_F = h/\mu$ (h is bottom depth and μ a linear drag coefficient) is longer than shear wave growth time scale (a few minutes). Both conditions are generally met in the real world but shear instability is difficult to observe and cannot be easily separated from extrinsic mechanisms of variability (Feddersen, 2014).

Numerical models predict that shear eddies have a strong impact on the time mean velocity profile due to momentum mixing across the longshore current. The mean velocity must therefore appear broader than the surfzone where it is generated. As a result, eddy activity is expected to affect the quality of littoral drift estimates. In this paper, we provide an original measure of mean longshore current inverted from video camera and compare it with a tridimensional (3D) model simulation for

DOI: 10.2112/SI75-082.1 received 15 October 2015; accepted in revision 15 January 2016.
*Corresponding author: Patrick.Marchesiello@ird.fr

the morning of March 11 2014. We analyze the characteristics and impact of shear waves and eddies on the mean flow and shed new light on the turbulent regime of nearshore flows.

METHODS

Grand Popo beach is located in the Gulf of Guinea, midway (80 km) between Cotonou (Benin) and Lome (Togo). Grand Popo is representative of the Bight of Benin as an open, wave-dominated and microtidal environment (0.3/1.8 m for neap/spring tidal ranges) exposed to S-SW long period swells generated at high latitudes in the South Atlantic. We chose the morning of March 11 2014 for our model-data comparison. The weather, tides and wave conditions were ideal: weak winds and wind waves well separated from a narrow-band swell of Hs=1.15 m, Tp=11 s, 10° incidence from shore normal direction (Figure 1). The water was at mid neap tide level (low-tide terrace at 80 cm depth), promoting a narrow surfzone less than 50 m wide starting seaward of the terrace.

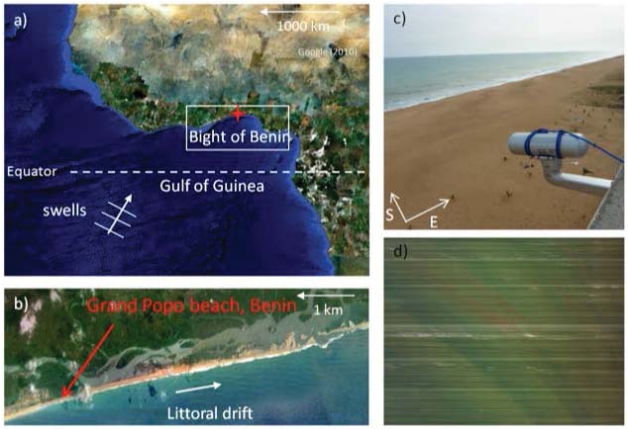

Figure 1. Study site and video camera. a) the Bight of Benin coast, with a red cross indicating the study site at Grand Popo; b) Grand Popo beach with evidence of oblique long swell producing longshore drift; c) HF video camera installed in Grand Popo; d) Secondary image from the video system: example of alongshore timestack used to estimate longshore flow velocity.

Coastal video

Field experiments conducted at Grand Popo beach in February 2013 (Almar *et al.*, 2014) and March 2014 were designed to monitor the beach and test the applicability of a low-cost video monitoring system (Figure 1). An Acoustic Doppler Current Profiler (ADCP) was moored in 10-m depth where incident waves were also measured. Surfzone currents were estimated by means of drifters deployed during daytime.

As opposed to in situ measurement techniques, remote sensing can safely provide synoptic coverage of the nearshore system over large areas and a wide range of scales. The profile of breaker dissipation can be assessed as in Flores *et al.* (2013) by estimating roller wavelength rather than light intensity. This method relying on energy conservation provides a safer means of calibrating the model wave forcing (Marchesiello *et al.*, 2015). Recently, a new method was also proposed for estimating longshore currents from video images (Larnier *et al.*, 2014). A Radon transform is applied on longshore timestacks to estimate the drift of foam or suspended particle signature in video images. The drifting angle gives an estimate of the longshore component of surface currents. Video estimations are validated for Grand Popo using drifters and ADCP measurements. It shows generally good agreement both in the surf and innershelf regions during 11-18 March 2014 (Figure 2). Offshore currents are about 10-20 cm/s while surfzone currents are much larger around 50 cm/s in average. Validation for March 11 is missing in the surfzone and we rely on the general agreement shown the rest of the week.

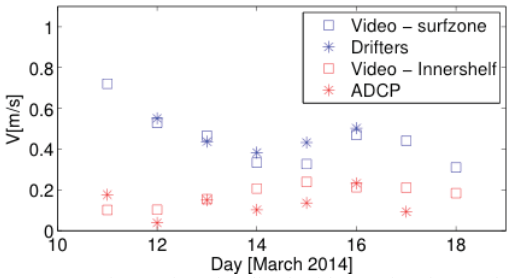

Figure 2. Comparison of co-localized video estimation and in-situ measurements of longshore currents in the surfzone (red) and innershelf (blue).

Wave-current model

Uchiyama *et al.* (2010) implemented a modeling approach for 3D wave-current interactions based on vortex-force formalism (McWilliams *et al.*, 2004) in the Regional Oceanic Modeling System (ROMS; Shchepetkin and McWilliams, 2005). Marchesiello *et al.* (2015) followed with the same approach within ROMS-AGRIF (Debreu *et al.*, 2012), allowing nesting and wetting/drying.

Eulerian wave-averaged current equations for mass, momentum, and tracers are included, plus non-conservative wave effects such as wave breaking. The currents are coupled with a ray-theory spectrum-peak wave propagation model (WKB model) describing wave crest conservation with wave refraction and conservation of both wave and roller action. The wave model includes dissipation due to shoaling-induced wave breaking and bottom drag and the Doppler-shifted current effect on waves. The latter was shown to lessen the destabilization of longshore currents (Ozkan-Haller and Li, 2003; Uchiyama *et al.*, 2009).

The observed water level, wind and wave conditions of Grand Popo beach were imposed at the offshore and surface boundaries of the coupled model. The domain size is 800 m longshore and 600 m cross-shore with a horizontal resolution of 3 m, time step of 0.3 seconds and 10 vertical levels. Periodic conditions are imposed at the cross-shore boundaries and radiative conditions at the offshore boundary (Marchesiello *et al.*, 2001). Because nearly all longshore current modeling in the literature uses shallow-water (2D) equations (one exception is Newberger and Allen, 2007, with mixed success), our 3D model is compared here with an equivalent 2D version of ROMS.

Model initialization

The model is first spun-up for 30 min without flow perturbation to reach a state where the longshore current speed V_0 is in balance between breaker acceleration and bottom drag

(Longuet-Higgins, 1970). Then, a small flow perturbation is superimposed on V_0 to initiate shear waves. From that point, the model is integrated for 10 hours.

The use of a linear bottom drag with coefficient $\mu \sim 3.10^{-3}$ m/s gives a forced current peak velocity $V_0 \sim 1.6$ m/s. It provides the best model-data agreement for mean and eddy signals. Sensitivity experiments with smaller or greater values lead to a mean current that is either too strong and wide or too weak and narrow.

Wave energy dissipation rate ε_b due to depth-induced breaking is computed in the wave model following Church and Thornton (1993). This parameterization works well for narrow-banded wave forcing provided that two empirical constants are known: the breaking wave parameter γ_b, and B_b accounting for the type of breaker. We achieve calibration of these parameters by comparing model-data dissipation patterns, assuming common scaling by V_0 (Figure 3; cyan curves). Values of 0.4 and 1.3, for γ_b and B_b respectively, provide the best fit to observation. The two curves feature a narrow surfzone starting at ~2 m depth seaward of the low-tide terrace. Closer to shore, the wave model misses some breaker dissipation that we attribute to wind waves with little impact on the longshore current.

RESULTS

We present results on the differences between the forced surfzone jet and resulting mean longshore flow. We then proceed to describe the mechanisms of shear wave and eddy productions that may explain the observed and modeled eddy effect.

Shear waves

The frequency f, wavelength λ, growth rate σ_i and phase speed c_p of unstable shear waves rely essentially on the mean current shear V_x and jet width Lj. From a linear stability analysis, Bowen and Holman (1989) propose simple relations for the most unstable waves: $f = 0.07V_x$, $\lambda = 2.5Lj$, $\sigma_i = 0.15V_x$ and $c_p = 0.25\text{-}0.5\ V_0$. For a narrow, shoreline-intensified jet typical of Grand Popo at mid-tide (Lj ~ 50m), shear can be strong. It is about 0.05 s^{-1} for the forced currents but weakens due to eddy mixing (Noyes *et al.*, 2004, argue from observations that shear waves stem from the forced rather than mean current). This implies a minimum shear wave period of about 5 min and wavelength of 125 m. Frictional spindown time for $\mu \sim 3.10^{-3}$ m/s is 5-10 min in the surfzone, *i.e.*, much longer than the growth time scale $\sigma^{-1} \sim 3$ min and thus favorable to their amplification.

To better assess the characteristics of linear most unstable waves, we ran the model with a large drag coefficient ($\mu = 6.10^{-3}$ m/s). In this weakly nonlinear regime, shear waves develop clear energy peaks at a period of 7 min and wavelength of 130 m (illustrated in Figure 3, left panel) and propagate along the flow with phase speed ~55 cm/s (estimated from a radon transform).

Shear eddies

When bottom drag is more realistic, shear waves with similar characteristics first develop but the flow becomes rapidly turbulent (center/right panels of Figure 3) with eddy kinetic energy representing 10-20 % of the mean. Eddies and filaments emerge on the seaward side of the jet, much like filaments observed with dye tracers (not shown). In this regime, the frequency spectrum broadens and the period in the surfzone is 4-10 min with modulation at larger periods (as in Allen *et al.*, 1996). In spite of coherency loss, the phase speed of propagation varies little over the simulation and is similar to the weakly nonlinear solution. This is expected from unstable modes that are approximately nondispersive (*e.g.*, Uchiyama *et al.*, 2009).

VLF variability was also computed from the video data on March 11 (3-hour period from 8 to 11 a.m. with fairly steady forcing conditions). Although these results are still preliminary, they indicate a standard deviation of longshore velocity of about 10 cm/s and a broad VLF frequency spectrum in agreement with the model. The VLF signal propagates only along the longshore current at ~ 50 cm/s, *i.e.*, much slower than gravity waves of the same frequency but very close to the model solution.

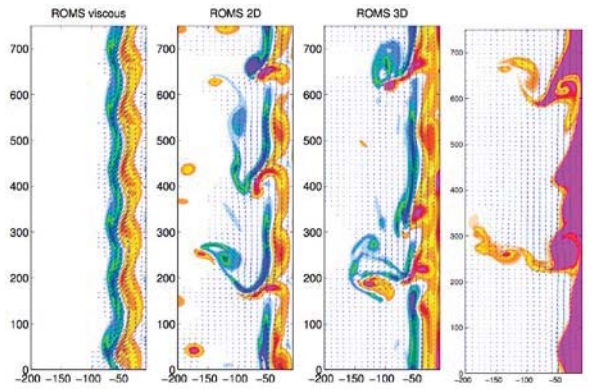

Figure 3. Instantaneous model vorticity and velocity vectors on the morning of March 11 2014. Left: shear waves developed from a 2D simulation with strong drag coefficient. Center: turbulent regime in 2D and 3D simulations with a realistic drag coefficient. Peak vorticity is 0.06 s^{-1}. The right panel shows a virtual dye released in the surfzone of the 3D simulation; it shows filaments and eddies ejecting seaward, much like aerial photos of dye experiments.

Eddy-mixed longshore flow

The forced longshore current profile used as initial flow in the model closely follows that of breaker dissipation. On the contrary, the time-mean longshore current profile (Figure 4; blue curves) is very broad in both model and data, extending more than 150 m offshore, well outside the surfzone. The model clearly reproduces the observed broadening of the current, although the peak velocity in the surfzone is larger in the model (about 1 m/s rather than 0.8 m/s).

Broadening of the model mean flow is due to cross-shore momentum mixing by shear waves and eddies. Eddy mixing is given by the cross-shore eddy advection term of the v equation: $A_t = -\langle u'v' \rangle_x$, where $-\langle u'v' \rangle$ is the time-mean cross-shore eddy flux of longshore flow v (Reynolds stress) and x the cross-shore distance. A_t has a strong decelerating effect in the surfzone (the depth-averaged value is ~ $1 m/s^2$, *i.e.*, half the bottom stress); it has an accelerating effect outside the surfzone (−0.5 m/s^2 balanced by the bottom stress) and vanishes at 150 m offshore (and toward the shoreline). The role of eddies is thus to extract large amounts of momentum from the longshore current in the

surfzone and spread it across. It should be noted that some redistribution of longshore current is also attributed to the vortex force and mean advection (Uchiyama *et al.*, 2009), but at a lesser degree here.

Another measure of eddy mixing is eddy viscosity: $\nu_t = -\langle u'v' \rangle / v_x$. Maximum values of ν_t are about 0.5 m^2/s seaward of the longshore current peak. Prandtl's mixing length-scale l defined by $\nu_t = l^2 v_x$ appears linearly dependent on |x| the distance to the shoreline (with coefficient ~ 0.075) in agreement with Longuet-Higgins (1970). This underlines that mixing is limited on the shoreward side of the current by the shoreline.

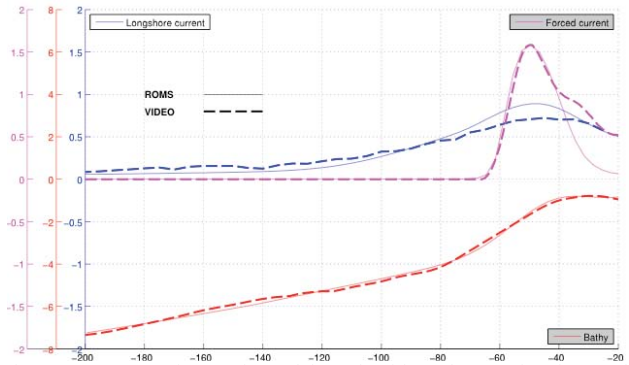

Figure 4. Comparison of model and video data estimations of bathymetry and longshore currents. The video (model) data is averaged over a 3-hour (10-hour) period and 250 (800) m alongshore distance. The forced current produced in the spinup phase of model simulation (cyan curve) has amplitude V_0 proportional to breaker dissipation and is used to scale dissipation from video data. The model bathymetry is an analytical fit to the video data.

DISCUSSION

It is generally assumed that nearshore dynamics follow a classical 2D turbulent regime (*e.g.*, Feddersen, 2014) but little evidence is found from the literature. To contribute on the subject in the context of longshore currents, we performed a wavenumber spectral analysis for 2D and 3D simulations (Figure 5). Consistently with 2D turbulence — in both 2D and 3D simulations — there is a strong inverse cascade of kinetic energy (KE) in the model starting from the scale of injection (~ 130 m). It should be noted that our 2D simulations produce more eddy energy at the same Reynolds number (same bottom drag) as expected from Squire's theorem and noted by Newberger and Allen (2007) for longshore currents. However, the injected energy travels more efficiently across the spectrum in the 3D model. Spectral fluxes are larger, *i.e.*, they promote the nonlinear growth of larger disturbances (compare the longshore scales in Figure 3b-c).

A sign of departure from 2D turbulence is the presence of a direct cascade (positive flux) downward from the injection scale. Here again, the flux is stronger in the 3D model. As a result, the 2D KE spectrum shows an energy deficit at both larger and smaller scales around the injection point (not shown). The 2D simulation has less direct KE flux but appears more efficient at downscaling enstrophy as in classical 2D turbulence (*e.g.* Figure 3b-c shows more numerous small-scale vortical flows in the 2D model). However, in all cases the KE spectra do not strictly follow any inertial slope (k^3 or $k^{-5/3}$), presumably due to the continuous effect of bottom friction across the spectrum. We conclude that the turbulent regime of nearshore regions is not properly explained by classical paradigms and deserves further investigation.

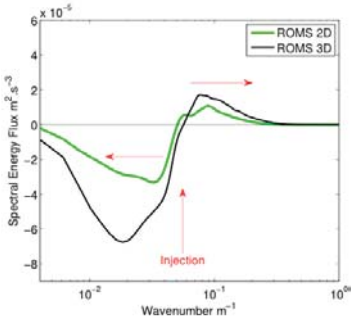

Figure 5. Left: Model (10-hour data) and video (3-hour data) frequency spectra of longshore velocity variance in the surfzone. Right: 3D and 2D model wavenumber spectral flux in the surf and innershelf regions. Vertical red arrows point to the period and wavenumber of most linearly unstable shear waves (7 min, 130 m) obtained from a viscous 2D simulation. The spectral flux is computed as in Marchesiello *et al.* (2011) by spectral integration of v advection term. Horizontal red arrows indicate positive/negative fluxes, *i.e.*, direct/inverse energy cascade toward smaller/larger scales.

CONCLUSIONS

The literature has long suggested a link between shear-flow instability of longshore currents and their mean cross-shore profile. Yet, recent investigations give increasing credit to extrinsic mechanisms of instantaneous wave forcing to explain the observed variability. Our results on Grand Popo beach based on video observation and model simulations provide further details on the 3D dynamics of strong longshore currents. They show that its broad mean profile is consistent with shear instability, conversion of mean to eddy kinetic energy and eddy mixing of momentum.

Our results reinforce the idea that between wave-driven surfzone circulation and wind-driven shelf circulation exist a transition zone in the innershelf region populated by filaments and eddies. Their horizontal scales are much larger than vertical ones but their turbulent dynamics do not clearly fit in the classical 2D paradigm since part of their energy fluxes down to smaller scales.

Instabilities in a 3D coupled wave-current model tend to generate less variance than the classical 2D uncoupled system (*e.g.*, Newberger and Allen, 2007) for two reasons. First, the feedback of rip currents on the incoming wave field is negative and thus reduces instability development (Uchiyama *et al.*, 2009; Yu and Slinn, 2003). Second, a shear flow is less unstable to 3D than 2D disturbances at the same Reynolds number, *i.e.*, with the same bottom drag (Squire's theorem). 3D longshore currents may thus be closer to the stability region and more often require stochastic excitation to generate variance (Farrell and

Ioannou, 1993). Stochastic forcing can lower the dependence of amplification on the Reynolds number. In this sense, intrinsic and extrinsic modes of variability should not be opposed but considered in future research as possibly interacting processes.

ACKNOWLEDGMENTS

This research has received support from French grants through ANR (COASTVAR: ANR-14-ASTR-0019; COMODO: ANR-11-MONU-005) and EC2CO/LEFE (Grand Popo Experiment and COMODO-WAVES). The fieldwork data in this study has been acquired by the authors and the source code for the model used, ROMS-AGRIF, is freely available (www.romsagrif.org).

LITERATURE CITED

Allen, J.S.; Newberger, P.A., and Holman, R.A., 1996. Nonlinear shear instabilities of alongshore currents on plane beaches. *J. Fluid Mech.*, 310, 181–213.

Almar, R., *et al.*, 2014. The Grand Popo beach 2013 experiment, Benin, West Africa: from short timescale processes to their integrated impact over long-term coastal evolution. *J. Coastal Res.*, 70, 651–656.

Bowen, A.J., and Holman, R.A., 1989. Shear instabilities of the mean longshore current: 1. Theory. *J. Geophys. Res.*: *Oceans*, 94 (C12), 18,023–18,030.

Church, J.C., and Thornton, E.B., 1993. Effects of breaking wave induced turbulence within a longshore current model. *Coastal Eng.*, 20, 1-28.

Clark, D.B., Elgar, S., and Raubenheimer, B., 2012. Vorticity generation by short-crested wave breaking. *Geophys. Res. Lett.*, 39 (L24604).

Debreu, L., Marchesiello, P.; Penven, P., and Cambon, G., 2012. Two-way nesting in split- explicit ocean models: Algorithms, implementation and validation. *Ocean Model.*, 49-50, 1-21.

Dodd, N.; Oltman-Shay, J., and Thornton E.B., 1992. Shear instabilities in the longshore current: A comparison of observation and theory. *J. Phys. Oceanogr.*, 22, 62–82.

Farrell, B.F., and Ioannou, P.J., 1993. Stochastic forcing of perturbation variance in unbounded shear and deformation flows. *J. Atmos. Sci.*, 50, 200–211.

Feddersen, F., 2014. The generation of surfzone eddies in a strong alongshore current. *J. Phys. Oceanogr.*, 44, 600–617.

Flores, R.P., Catalan, P.A, and Haller, M.C., 2013. Incorporating remotely-sensed roller properties into set-up estimations for random wave conditions, in Proceedings of Coastal Dynamics 2013, 615-626, Nantes, France.

Kaki, C., Laibi, R.A,, and Oyede, L.M., 2011. Evolution of beninese coastline from 1963 to 2005: Causes and consequences. *Br. J. Env. Clim. Change*, 1, 216–231.

Laibi, R.A.; Anthony, E.J.; Almar, R.; Castelle, B.; Senechal, N., and Kestenar, E., 2014. Longshore drift cell development on the human-impacted Bight of Benin sand barrier coast, West Africa. *J. Coast. Res.*, 70, 78–83.

Larnier, S.; Almar, R.; Cienfuegos, R., and Lejay, A., 2014. On the use of the radon transform to estimate longshore currents from video imagery. *J. Coast. Res.*, 70, 23–28.

Longuet-Higgins, M. S., 1970. Longshore currents generated by obliquely incident sea waves: 2. *J. Geophys. Res.*, 75, 6790–6801.

Marchesiello, P.; McWilliams, J.C., and Shchepetkin, A., 2001. Open boundary conditions for long-term integration of regional oceanic models. *Ocean Model.*, 3, 1-20.

Marchesiello, P.; Capet, X.; Menkes, C., and Kennan, S.C., 2011. Submesoscale dynamics in tropical instability waves. *Ocean Model.*, 39, 31–46.

Marchesiello, P.; Benshila, R.; Almar, R.; Uchiyama, Y.; McWilliams, J.C., and Shchepetkin, A., 2015. On tridimensional rip current modeling. *Ocean Model.*, doi:10.1016/j.ocemod.2015.07.003.

McWilliams, J.C., Restrepo, J.M., and Lane, M.R., 2004. An asymptotic theory for the interaction of waves and currents in coastal waters. *J. Fluid Mech.*, 511, 135–178.

Newberger, P.A., and Allen, J.S., 2007. Forcing a three-dimensional, hydrostatic, primitive-equation model for application in the surf zone: 2. application to duck94. *J. Geophys. Res.*: *Oceans*, 112(C8).

Noyes, T.J.; Guza R.T.; Elgar, S., and Herbers, T.H.C., 2004. Field observations of shear waves in the surf zone. *J. Geophys. Res.*, 109 (C01031).

Oltman-Shay, J.; Howd, P.A., and Birkemeier, W.A., 1989. Shear instabilities of the mean longshore current: 2. field observations. *J. Geophys. Res.: Oceans*, 94 (C12), 18,031–18,042.

Oskan-Haller, H.T., and Li, Y., 2003. Effects of wave-current interaction on shear instabilities of longshore currents. *J. Geophys. Res.: Oceans*, 108 (C5).

Peregrine, D.H., 1998. Surf zone currents. *Theor. Comput. Fluid Dyn.*, 10, 295–309.

Shchepetkin, A.F., and McWilliams, J.C., 2005. The regional oceanic modeling system (ROMS): a split-explicit, free-surface, topography-following-coordinate oceanic model. *Ocean Model.*, 9, 347-404.

Slinn, D.N.; Allen, J.S.; Newberger, P.A., and Holman, R.A., 1998. Nonlinear shear instabilities of alongshore currents over barred beaches. *J. Geophys. Res.*, 103 (C9), 18,357-18,379.

Uchiyama, Y.; McWilliams, J.C., and Restrepo, J.M., 2009. Wave-current interaction in nearshore shear instability analyzed with a vortex force formalism. *J. Geophys. Res.: Oceans*, 114 (C6).

Uchiyama, Y.; McWilliams, J.C., and Shchepetkin, A., 2010. Wave-current interaction in an oceanic circulation model with a vortex-force formalism: Application to the surf zone. *Ocean Model.*, 34, 16–35.

Yu, J., and Slinn, D.N., 2003. Effects of wave-current interaction on rip currents. *J. Geophys. Res.: Oceans*, 108(C3).